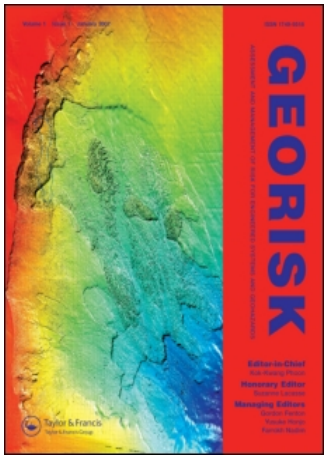

Georisk: Assessment and Management of Risk for Engineered Systems and Geohazards
Publication details, including instructions for authors and subscription information:
http://www.informaworld.com/smpp/title~content=t744347545

Reliability of shallow foundations designed against bearing failure using LRFD

Gordon A. Fenton [a]; Xianyue Zhang [b]; D. V. Griffiths [c]
[a] Department of Engineering Mathematics, Dalhousie University, Halifax, Nova Scotia, Canada
[b] Jacques Whitford, Calgary, Alberta, Canada
[c] Division of Engineering, Colorado School of Mines, Golden, CO, USA

Online Publication Date: 01 December 2007
To cite this Article: Fenton, Gordon A., Zhang, Xianyue and Griffiths, D. V. (2007) 'Reliability of shallow foundations designed against bearing failure using LRFD', Georisk: Assessment and Management of Risk for Engineered Systems and Geohazards, 1:4, 202 - 215
To link to this article: DOI: 10.1080/17499510701812844
URL: http://dx.doi.org/10.1080/17499510701812844

Georisk, Vol. 1, No. 4, December 2007, 202–215

Taylor & Francis
Taylor & Francis Group

Reliability of shallow foundations designed against bearing failure using LRFD

GORDON A. FENTON*†, XIANYUE ZHANG‡ and D. V. GRIFFITHS¶

†Department of Engineering Mathematics, Dalhousie University, Halifax, Nova Scotia, Canada B3J 2X4
‡Jacques Whitford, 805-8th Avenue SW, Suite 300, Calgary, Alberta, Canada T2P1H7
¶Division of Engineering, Colorado School of Mines, Golden, CO 80401-1887, USA

Worldwide, there is growing interest in the development of a rational reliability-based geotechnical design code. The reasons for this interest are at least two-fold; first, geotechnical engineers face significantly more uncertainties than those faced in other fields of engineering, therefore there is a need to properly characterize and deal with these uncertainties. Second, for decades, structural engineers have used a reliability-based design code, and there is a need to develop the same for geotechnical engineers, in order that the two groups can 'speak the same language'. This paper develops a theoretical model to predict the probability that a shallow foundation will exceed its supporting soil's bearing capacity. The footing is designed using characteristic soil properties (cohesion and friction angle) derived from a single sample, or 'core', taken in the vicinity of the footing, and used in a load and resistance factor design approach. The theory predicting failure probability is validated using a two-dimensional random finite element method analysis of a strip footing. Agreement between theory and simulation is found to be very good. Therefore, the theory can be used with confidence to perform risk assessments of foundation designs and develop resistance factors for use in code provisions.

Keywords: Bearing capacity; Risk assessment; Load and resistance factor design; Ultimate limit state; Shallow foundation

1. Introduction

When designing a shallow foundation, the designer faces a variety of uncertainties. For example, the load applied to the footing will have some uncertainty associated with it, and the ground supporting the footing will not be perfectly understood. For this reason, there will always be some risk that the footing will experience a bearing capacity failure. It is the responsibility of the designer to ensure that the risk of bearing capacity failure is sufficiently small. This paper develops a theoretical tool that can be used to estimate the probability of bearing capacity failure of shallow foundations. The theory is based on a theoretical and simulation-based study by Zhang (2007).

The shallow foundations are assumed to follow a design process that initially involves determining the characteristic load that the footing is to support. Then, the ground at the site is investigated to establish characteristic soil properties for use in the bearing capacity prediction model. Finally, the footing dimensions are determined in order to satisfy the following load and resistance factor design (LRFD) equation

$$\phi_g \hat{R}_u \geq I[\alpha_L \hat{L}_L + \alpha_D \hat{L}_D], \tag{1}$$

where ϕ_g is the geotechnical resistance factor, $\hat{R}_u$ is the ultimate geotechnical resistance based on characteristic soil properties, I is an importance factor, $\hat{L}_L$ is the characteristic

*Corresponding author: E-mail: gordon.fenton@dal.ca

Georisk
ISSN 1749-9518 print/ISSN 1749-9526 online
http://www.tandf.co.uk/journals
DOI: 10.1080/17499510701812844

live load, $\hat{L}_D$ is the characteristic dead load, and α_L and α_D are the live and dead load factors, respectively. Only dead and live loads are considered in this paper, although the results are easily extended to other load combinations. The load factors used in this paper will be as specified by the National Building Code of Canada (NBCC 2006); $\alpha_L = 1.5$ and $\alpha_D = 1.25$. It is noted that the purpose of this paper is not to validate any recommendations the National Building of Canada may have on geotechnical design, but to develop a model which can be subsequently used to find the resistance factors required for the ultimate limit state design of a shallow foundation (see Fenton *et al*. 2007).

The ultimate geotechnical resistance, R_u, is determined using characteristic soil properties, in this case the characteristic values of the soil's cohesion, c, and friction angle, ϕ (note that primes are omitted from these quantities simply because any definitions for cohesion and friction that lead to a reasonable approximation of bearing capacity are acceptable). The characteristic values are defined here as the median of the sampled observations of c and the arithmetic average of the sampled observations of ϕ at the site. These choices are made to simplify their distributions and will be assumed to be the characteristic values used in the design process, as proposed by Fenton *et al*. (2007). The importance factor, I, reflects the severity of the failure consequences, and may be larger than 1.0 for important structures, such as hospitals, whose failure consequences are severe and whose target probabilities of failure are much less than for typical structures. Typical structures are usually designed using $I = 1$, which will be assumed in this paper. Structures with low failure consequences (minimal risk of loss of life, injury and/or economic impact) may have $I < 1$.

If the soil is assumed weightless, the computation of the ultimate bearing stress, q_u, simplifies to:

$$q_u = cN_c. \tag{2}$$

The assumption that the soil is weightless is conservative since the soil weight contributes to the overall bearing capacity and allows this study to concentrate solely on the effect of spatial variability of the soil on failure probability. The ultimate geotechnical resistance, R_u, is the product of q_u and the footing area. Since the theory developed here is validated using a two-dimensional simulation of a soil supporting a strip footing, R_u in this paper is computed as:

$$R_u = Bq_u = BcN_c, \tag{3}$$

which has units of force per unit length of the strip footing out-of-plane (i.e. in the direction of the strip). Two forms of equation (3) will be considered in this paper; one will be the design equation, $\hat{R}_u$, which is based on characteristic soil parameters, $\hat{c}$ and $\hat{\phi}$, and the other will be the true (random) R_u of a strip footing placed on a spatially variable soil.

The N_c factor is generally determined using plasticity theory (see, e.g. Prandtl 1921, Terzaghi 1943, Sokolovski 1965) in which a rigid base punches into a softer material. The theories presented by these authors assume that the soil underlying the footing has properties that are spatially constant (everywhere the same). Henceforth, this type of ideal soil will be referred to as a *uniform soil*. Under this assumption, most bearing capacity theories (e.g. Prandtl 1921, Meyerhof 1951, 1963) assume that the failure slip surface takes on a logarithmic spiral shape to give:

$$N_c = \frac{e^{\pi \tan\phi} \tan^2\left(\frac{\pi}{4} + \frac{\phi}{2}\right) - 1}{\tan\phi}. \tag{4}$$

It is hypothesized in this paper that equivalent soil parameters, $\bar{c}$ and $\bar{\phi}$ (and thus $\bar{N}_c$), can be found such that a uniform soil having parameters $\bar{c}$ and $\bar{\phi}$ will have the same bearing capacity as the actual bearing capacity of the spatially variable soil. If $\bar{c}$ and $\bar{\phi}$ are known, then equation (3) can be modified as follows to determine the true ultimate geotechnical resistance of the footing,

$$R_u = B\bar{c}\bar{N}_c, \tag{5}$$

where $\bar{N}_c$ is the equivalent N_c factor which is obtained by using the equivalent friction angle $\bar{\phi}$ in equation (4),

$$\bar{N}_c = \frac{e^{\pi \tan\bar{\phi}} \tan^2\left(\frac{\pi}{4} + \frac{\bar{\phi}}{2}\right) - 1}{\tan\bar{\phi}}. \tag{6}$$

Characteristic soil properties are determined by taking m samples of the soil near the footing, and using some sort of average of the observed soil properties. For example, the soil sample could be a CPT sounding or a core (both called vertical samples) taken at a distance r from the footing centerline. Only one such vertical sample will be considered in this paper – if vertical samples are well spaced horizontally, the sample closest to the footing location should be used. Of course, more than one vertical sample may be available, in which case the site understanding is increased and the failure probabilities predicted here would be conservative. It is pointed out that there are several assumptions made in this paper, most conservative, but some unconservative. These assumptions will be enumerated and discussed in the conclusions.

From the m samples, the characteristic cohesion, $\hat{c}$, is assumed to be the *median* of the samples. The median can be computed by ordering the samples, $c_1^o, c_2^o, \ldots, c_m^o$, where c_i^o denotes an *observed* cohesion value, from the smallest to the largest, and then using the classical median estimator:

$$\hat{c} = \begin{cases} c^o_{(m+1)/2} & \text{if } m \text{ is odd} \\ \dfrac{1}{2}(c^o_{m/2} + c^o_{1+m/2}) & \text{if } m \text{ is even} \end{cases}. \tag{7}$$

If c is lognormally distributed, as assumed here, an equivalent (in mean) estimate of the median involves a multiplicative form that is the geometric average:

$$\hat{c} = \left[\prod_{i=1}^{m} c_i^{\circ}\right]^{1/m} = \exp\left\{\frac{1}{m}\sum_{i=1}^{m} \ln c_i^{\circ}\right\}, \tag{8}$$

which is the mth root of the product of the observed values. There are two advantages to the latter multiplicative form of the median estimator; first, it is easier to see that equation (8) is dominated by low values of c_i° – e.g. if any $c_i^{\circ} = 0$, then $\hat{c} = 0$; and second, it can be shown that $\hat{c}$ will tend to a lognormal distribution by the Central Limit Theorem (taking the natural logarithm of both sides of equation (8) leads to a *sum* of random variables on the right-hand-side which the Central Limit Theorem says will tend to a normal distribution). The median estimate given by equation (8) is used in this paper.

The friction angle will be assumed to follow a symmetric and bounded distribution, as discussed next. As the distribution is symmetric, an arithmetic average is selected to define the characteristic friction angle, $\hat{\phi}$, simply because the arithmetic average preserves the mean of the distribution. In this case, the characteristic friction angle is defined as:

$$\hat{\phi} = \frac{1}{m}\sum_{i=1}^{m} \phi_i^{\circ}, \tag{9}$$

where ϕ_i° are the friction angles observed (sampled) at the site. It is assumed that both the cohesion and friction angle observations are taken from the same set of samples, i.e. that each sample, $i = 1,2, \ldots m$ yields both a friction angle (ϕ_i°) and a cohesion (c_i°) observation.

Using the characteristic soil properties, the design ultimate geotechnical resistance becomes:

$$\hat{R}_u = B\hat{c}\hat{N}_c, \tag{10}$$

where

$$\hat{N}_c = \frac{e^{\pi\tan\hat{\phi}}\tan^2\left(\frac{\pi}{4}+\frac{\hat{\phi}}{2}\right) - 1}{\tan\hat{\phi}}. \tag{11}$$

The determination of the probability of bearing capacity failure now involves determining the joint distributions of the load, the 'as-sampled' characteristic soil properties ($\hat{c}$ and $\hat{N}_c$), and the true equivalent soil properties ($\bar{c}$ and $\bar{N}_c$).

2. The random soil model

The soil cohesion, c, is assumed to be lognormally distributed with mean μ_c, standard deviation σ_c, and spatial correlation length $\theta_{\ln c}$. A lognormally distributed random field is obtained from a normally distributed random field, $G_{\ln c}(\underline{x})$, having zero mean, unit variance, and spatial correlation length $\theta_{\ln c}$ through the transformation:

$$c(\underline{x}) = \exp\{\mu_{\ln c} + \sigma_{\ln c} G_{\ln c}(\underline{x})\}, \tag{12}$$

where $\underline{x}$ is the spatial position at which c is desired, $\sigma_{\ln c}^2 = \ln(1+V_c^2)$, $\mu_{\ln c} = \ln(\mu_c) - \sigma_{\ln c}^2/2$, and $V_c = \sigma_c/\mu_c$ is the cohesion's coefficient of variation.

The correlation coefficient between the log-cohesion at a point $\underline{x}_1$ and a second point $\underline{x}_2$ is specified by a correlation function, $\rho_{\ln c}(\underline{\tau})$, where $\underline{\tau} = \underline{x}_1 - \underline{x}_2$ is the vector between the two points. A simple exponentially decaying (Markovian) correlation function will be assumed having the form:

$$\rho_{\ln c}(\underline{\tau}) = \exp\left(-\frac{2|\underline{\tau}|}{\theta_{\ln c}}\right), \tag{13}$$

where $|\underline{\tau}|$ is the length of the vector $\underline{\tau}$. The spatial correlation length, $\theta_{\ln c}$, is loosely defined as the separation distance within which two values of $\ln c$ are significantly correlated. Mathematically, $\theta_{\ln c}$ is defined as the area under the correlation function, $\rho_{\ln c}(\underline{\tau})$ (Vanmarcke 1984).

The spatial correlation function, $\rho_{\ln c}(\underline{\tau})$ has a corresponding variance reduction function, $\gamma_{\ln c}(D)$, which specifies how the variance is reduced upon local averaging of $\ln c$ over some domain D. In the two-dimensional analysis used to validate the theory, $D = D_1 \times D_2$ is an area and the two-dimensional variance reduction function is defined by:

$$\gamma_{\ln c}(D_1, D_2) = \frac{4}{(D_1 D_2)^2}\int_0^{D_1}\int_0^{D_2} (D_1 - \tau_1) \times (D_2 - \tau_2)\rho(\tau_1, \tau_2)d\tau_1 d\tau_2, \tag{14}$$

which can be evaluated using Gaussian quadrature (see, e.g. Fenton and Griffiths 2003 and Griffiths and Smith 2006, for more details).

It should be emphasized that the correlation function selected above acts between values of $\ln c$. This is because $\ln c$ is normally distributed and a normally distributed random field is simply defined by its mean and covariance structure. In practice, the correlation length $\theta_{\ln c}$ can be estimated by evaluating spatial statistics of the log-cohesion data directly (see, e.g. Fenton 1999). Unfortunately, as such studies are scarce, little is currently known about the spatial correlation structure of natural soils. For the problem considered here, it turns out that a worst case correlation length exists which can be conservatively assumed in the absence of improved information.

The random field is also assumed in the simulations to be statistically isotropic (the same correlation length in any direction through the soil). Although the horizontal correlation length is often greater than the vertical due to soil layering, taking this into account was deemed to be a site specific refinement which does not lead to an increase in the general understanding of the probabilistic behavior of shallow foundations. The theory presented below, however,

is applicable to both isotropic and anisotropic fields, although only the isotropic case was validated.

The friction angle, ϕ, is assumed to be bounded both above and below, so that neither normal nor lognormal distributions are appropriate. A beta distribution is often used for bounded random variables. Unfortunately, a beta distributed random field has a very complex joint distribution, and simulation is cumbersome and numerically difficult. To keep things simple, a bounded distribution is selected which resembles a beta distribution but which arises as a simple transformation of a standard normal random field, $G_\phi(\underline{x})$, according to:

$$\phi(\underline{x}) = \phi_{\min} + \frac{1}{2}(\phi_{\max} - \phi_{\min})\left\{1 + \tanh\left(\frac{sG_\phi(\underline{x})}{2\pi}\right)\right\}, \quad (15)$$

where $\phi_{\min}$ and $\phi_{\max}$ are the minimum and maximum friction angles in radians, respectively, and s is a scale factor which governs the friction angle variability between its two bounds. Figure 1 shows how the distribution of ϕ (normalized to the interval [0, 1]) changes as s changes, going from an almost uniform distribution at $s=5$ to a very normal looking distribution for smaller s. Thus, varying s between about 0.1 and 5.0 leads to a wide range in the stochastic behavior of ϕ. In all cases, the distribution is symmetric so that the midpoint between $\phi_{\min}$ and $\phi_{\max}$ is the mean. Values of s greater than about 5 lead to a U-shaped distribution (higher at the boundaries), which is deemed unrealistic.

The following relationship between s and the variance of ϕ derives from a third-order Taylor series approximation to tanh in the second line and a first-order approximation to the expectation in the third line:

$$\sigma_\phi^2 = (0.5)^2(\phi_{\max} - \phi_{\min})^2 \mathrm{E}\left[\tanh^2\left(\frac{sG_\phi}{2\pi}\right)\right]$$

$$\simeq (0.5)^2(\phi_{\max} - \phi_{\min})^2 \mathrm{E}\left[\frac{\left(\frac{sG_\phi}{2\pi}\right)^2}{1 + \left(\frac{sG_\phi}{2\pi}\right)^2}\right],$$

$$\simeq (0.5)^2(\phi_{\max} - \phi_{\min})^2 \frac{s^2}{4\pi^2 + s^2} \quad (16)$$

where $\mathrm{E}[G_\phi^2] = 1$, since G_ϕ is a standard normal random variable. Equation (16) slightly overestimates the true standard deviation of ϕ by 0% when $s=0$ to 11% when $s=5$. A much closer approximation over the entire range $0 \le s \le 5$ is obtained by slightly decreasing the 0.5 factor to 0.46 (this is an empirical adjustment),

$$\sigma_\phi \simeq \frac{0.46(\phi_{\max} - \phi_{\min})s}{\sqrt{4\pi^2 + s^2}} \quad (17)$$

The close agreement is illustrated in figure 2.

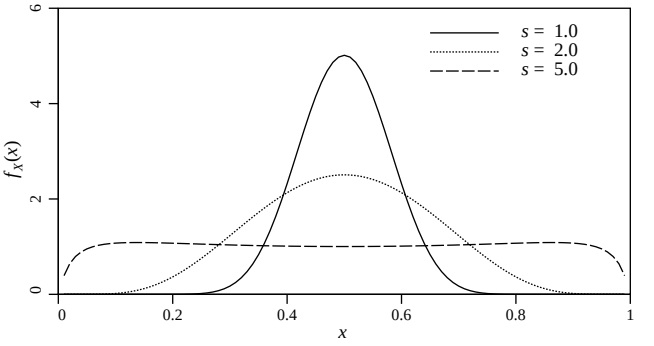

Figure 1. Bounded distribution of friction angle normalized to the interval [0,1].

Equation (16) can be generalized to yield the covariance between $\phi(\underline{x}_i)$ and $\phi(\underline{x}_j)$ for any two spatial points $\underline{x}_i$ and $\underline{x}_j$, as follows:

$$\mathrm{Cov}[\phi(\underline{x}_i), \phi(\underline{x}_j)]$$

$$= (0.5)^2(\phi_{\max} - \phi_{\min})^2 \mathrm{E}\left[\tanh\left(\frac{sG_\phi(\underline{x}_i)}{2\pi}\right) \tanh\left(\frac{sG_\phi(\underline{x}_j)}{2\pi}\right)\right]$$

$$\simeq (0.5)^2(\phi_{\max} - \phi_{\min})^2$$

$$\mathrm{E}\left[\frac{\left(\frac{sG_\phi(\underline{x}_i)}{2\pi}\right)\left(\frac{sG_\phi(\underline{x}_j)}{2\pi}\right)}{1 + \frac{1}{2}\left(\left(\frac{sG_\phi(\underline{x}_i)}{2\pi}\right)^2 + \left(\frac{sG_\phi(\underline{x}_j)}{2\pi}\right)^2\right)}\right],$$

$$\simeq (0.46)^2(\phi_{\max} - \phi_{\min})^2 \frac{s^2\rho_\phi(\underline{x}_i - \underline{x}_j)}{4\pi^2 + s^2}$$

$$= \sigma_\phi^2 \rho_\phi(\underline{x}_i - \underline{x}_j) \quad (18)$$

where the empirical correction found in equation (17) was introduced in the second last step.

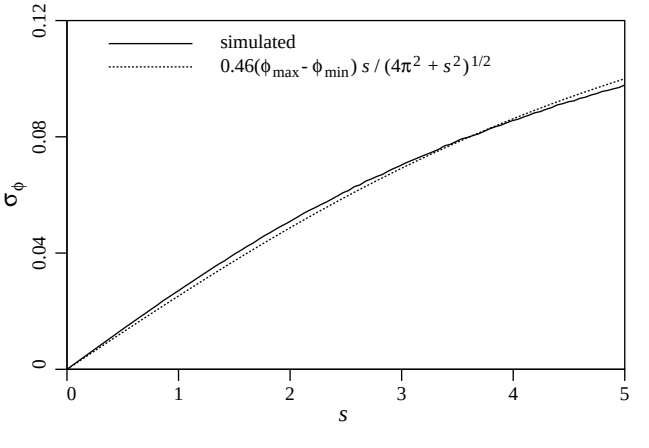

Figure 2. Relationship between σ_ϕ and s derived from simulation (100,000 realizations for each s) and the Taylor's series derived approximation given by equation (17). The vertical scale corresponds to $\phi_{\max}$–$\phi_{\min} = 0.349$ radians (20°).

It seems reasonable to assume that if the spatial correlation structure of a soil is caused by changes in the constitutive nature of the soil over space, then both the cohesion and friction angle would have similar correlation lengths. Thus, θ_ϕ is taken to be equal to $\theta_{\ln c}$ in this study, and ϕ is assumed to have the same correlation structure as c (equation 13), i.e. $\rho_\phi(\underline{\tau}) = \rho_{\ln c}(\underline{\tau})$. Both correlation lengths will be referred to generically from now on simply as θ, and both correlation functions as $\rho(\underline{\tau})$, remembering that this length and correlation function reflects correlation between points in the underlying normally distributed random fields, $G_{\ln c}(\underline{x})$ and $G_\phi(\underline{x})$, and not directly between points in the cohesion and friction fields (although the correlation lengths in the different spaces are actually quite similar). The correlation lengths can be estimated by statistically analyzing data generated by inverting equations (12) and (15). Since both fields have the same correlation function, $\rho(\underline{\tau})$, they will also have the same variance reduction function, i.e. $\gamma_{\ln c}(D) = \gamma_\phi(D) = \gamma(D)$, as defined by equation (14).

The two random fields, c and ϕ, are assumed independent. Fenton and Griffiths (2003) found that the non-zero correlations between c and ϕ have only a minor influence on the estimated probabilities of bearing capacity failure. Since the general consensus is that c and ϕ are negatively correlated (Wolff 1985, Cherubini 2000) and the mean bearing capacity for independent c and ϕ was slightly lower than for the negatively correlated case (Fenton and Griffiths 2003), the assumption of independence between c and ϕ is slightly conservative. However, the difference is minor, and is not deemed a major source of conservatism.

3. The random load model

The load acting on the footing is assumed composed of a live load component and a dead load component. The dead load component is relatively static over the lifetime of the supported structure, and is assumed to have a fixed (non-time varying) lognormal distribution with mean μ_D and standard deviation σ_D.

The definition of live load is somewhat more complicated than that of dead load, since live loads change dynamically with time. Live loads used in design are based on the maximum (extreme) live load experienced by the structure over the structure's lifetime. Since the maximum live load observed over the first year of service is likely to be significantly less than that observed over the first 100 years of service, it is apparent that the distribution of the maximum live load depends on the assumed lifetime. The maximum live load experienced by the footing will be denoted L_{Le}, the subscript 'e' implying 'extreme'. It is assumed that L_{Le} is also lognormally distributed with mean μ_{Le} and standard deviation σ_{Le}. Figure 3 illustrates the difference between the maximum lifetime live load and the instantaneous 'any time' live load distributions. Also shown is the dead load distribution. Although the true distribution of the live load is more likely to be an extreme value distribution, the lognormal distribution is a conservative assumption, in that it has a heavier upper tail, which leads to a tractable solution in the following. In any case, the total load acting on the footing will be the sum of a lognormal dead load and an extreme value live load. The resulting distribution will be a mixture of lognormal and extreme value distributions – the lognormal distribution is a reasonable approximation to this mixture.

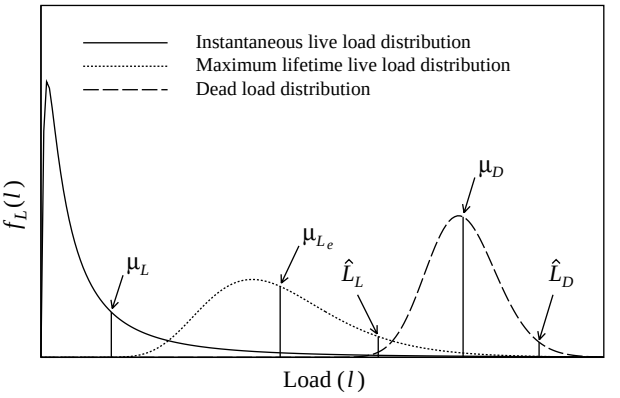

Figure 3. Instantaneous live, maximum lifetime live, and dead load distributions.

The characteristic design loads, also shown in figure 3, will be assumed defined in terms of the means of the load components in the following fashion:

$$\hat{L}_L = k_{L_e}\mu_{L_e} \tag{19a}$$

$$\hat{L}_D = k_D\mu_D, \tag{19b}$$

where μ_{Le} and μ_D are the means of the live and dead loads, respectively, and k_{Le} and k_D are live and dead load *bias* factors, respectively. The bias factors provide some degree of 'comfort' by increasing the loads from the mean value to a value having a lesser chance of being exceeded. The locations of the characteristic design loads, relative to their distributions, are illustrated in figure 3.

For typical multi-story office buildings, Allen (1975) estimates $\mu_{Le} = 1.7$ kN/m^2, based on a 30-year lifetime. The corresponding characteristic live load given by the NBCC (2006) is $\hat{L}_L = 2.4$ kN/m^2, which implies that $k_{Le} = 2.4/1.7 = 1.41$. Dead load, on the other hand, is largely static, and the time span considered (e.g. lifetime) has little effect on its distribution. Becker (1996) estimates $k_D = 1.18$.

The total true load acting on the footing, L, is the sum of dead and maximum lifetime live loads:

$$L = L_D + L_{L_e}. \tag{20}$$

Since the sum of two lognormally distributed random variables does not have a simple closed form solution, for

simplicity it will be assumed here that L is also lognormally distributed with parameters:

$$\mu_L = \mu_D + \mu_{L_e},$$
$$\sigma_L^2 = \sigma_D^2 + \sigma_{L_e}^2,$$

where dead and live loads are assumed uncorrelated in the calculation of the variance of L.

Figure 4 illustrates how the assumed lognormal distribution of L agrees with simulation. To produce each figure, 1000 independent realizations of L_{Le} and L_D were simulated and added in equation (20) to obtain 1000 realizations of L. A frequency density plot of these realizations was then produced and a fitted lognormal distribution superimposed. The left plot (a) was produced assuming a dead to live load ratio $\mu_D/\mu_{Le} = 1.0$, while the right plot (b) assumed $\mu_D/\mu_{Le} = 3.0$. In both cases, the lognormal fit is seen as very reasonable. In fact, the p-value corresponding to the hypothesis test having null that the total load is lognormally distributed is 0.17 in (a) and 0.27 in (b). These large p-values support the hypothesis that the total load distribution is closely approximated by the lognormal distribution and this distribution will be adopted here.

4. Analytical approximation to the probability of failure

The design footing width, B, is obtained using equation (10) in equation (1), which, in terms of the characteristic soil properties becomes:

$$B = \frac{I[\alpha_L \hat{L}_L + \alpha_D \hat{L}_D]}{\phi_g \hat{c} \hat{N}_c}. \tag{21}$$

The probability of bearing capacity failure is the probability that the true footing load, L, exceeds the true bearing capacity, $q_u B$, where B is as designed in equation (21):

$$p_f = P[L > q_u B] = P[L > \bar{c} \bar{N}_c B]. \tag{22}$$

Substituting equation (21) into equation (22) and collecting random terms to the left of the inequality leads to:

$$p_f = P\left[L \frac{\hat{c}\hat{N}_c}{\bar{c}\bar{N}_c} > \frac{I[\alpha_L \hat{L}_L + \alpha_D \hat{L}_D]}{\phi_g}\right]. \tag{23}$$

Letting

$$Y = L \frac{\hat{c}\hat{N}_c}{\bar{c}\bar{N}c}, \tag{24}$$

means that

$$p_f = P\left[Y > \frac{I[\alpha_L \hat{L}_L + \alpha_D \hat{L}_D]}{\phi_g}\right], \tag{25}$$

and the task is to find the distribution of Y. Assuming that Y is lognormally distributed (an assumption that is supported to some extent by the central limit theorem), then:

$$\ln Y = \ln L + \ln \hat{c} + \ln \hat{N}_c - \ln \bar{c} - \ln \bar{N}_c, \tag{26}$$

is normally distributed and p_f can be found once the mean and variance of $\ln Y$ are determined. The mean of $\ln Y$ is

$$\mu_{\ln Y} = \mu_{\ln L} + \mu_{\ln \hat{c}} + \mu_{\ln \hat{N}_c} - \mu_{\ln \bar{c}} - \mu_{\ln \bar{N}_c} \tag{27}$$

and the variance of $\ln Y$ is

$$\sigma^2_{\ln Y} = \sigma^2_{\ln L} + \sigma^2_{\ln \hat{c}} + \sigma^2_{\ln \bar{c}} + \sigma^2_{\ln \hat{N}_c} + \sigma^2_{\ln \bar{N}_c} - 2\mathrm{Cov}[\ln \bar{c}, \ln \hat{c}] - 2\mathrm{Cov}[\ln \bar{N}_c, \ln \hat{N}_c] \tag{28}$$

where the load L, and soil properties c and ϕ are reasonably assumed to be mutually independent. To find the parameters in equations (27) and (28), the following assumptions are made.

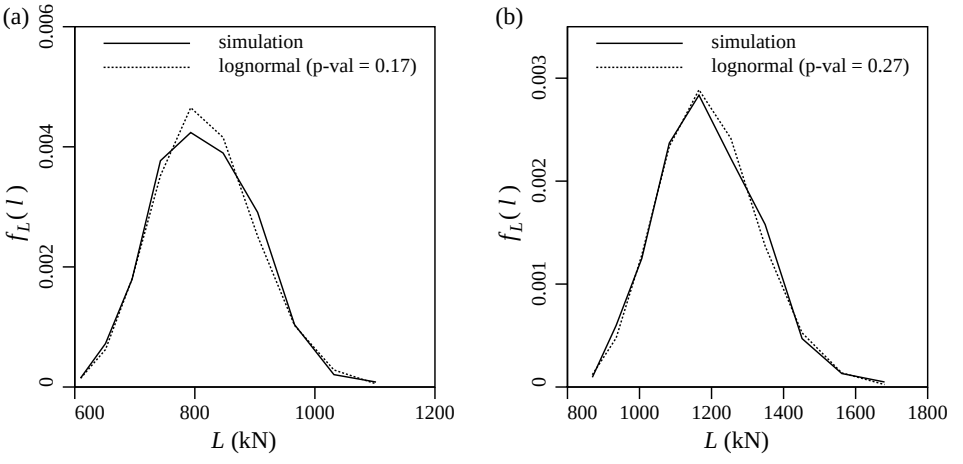

Figure 4. Comparison of simulated and fitted lognormal distribution for total load, L, with ratio of dead to live load of 1.0 in (a) and 3.0 in (b).

1. m error-free observations of the soil cohesion and friction angle have been obtained by site exploration. In this paper, it is assumed that these observations are extracted from a single boring, or sounding, taken near the footing.
2. The equivalent cohesion, $\bar{c}$, is the geometric average of the cohesion field over some zone of influence, D, under the footing:

$$\bar{c} = \exp\left\{\frac{1}{D}\int_D \ln c(\underset{\sim}{x})d\underset{\sim}{x}\right\}. \tag{29}$$

   In this two-dimensional analysis, D is an area and the above is a two-dimensional integration. If $c(\underset{\sim}{x})$ lognormally distributed, as assumed, then $\bar{c}$ is also lognormally distributed.
3. The equivalent friction angle, $\bar{\phi}$, is the arithmetic average of the friction angle over the zone of influence, D:

$$\bar{\phi} = \frac{1}{D}\int_D \phi(\underset{\sim}{x})d\underset{\sim}{x}. \tag{30}$$

   This relationship preserves the mean, i.e. $\mu_{\bar{\phi}} = \mu_{\phi}$.

Probably the greatest source of uncertainty in this theory involves the choice of the domain, D, over which the equivalent soil properties are averaged under the footing. The averaging domain was found by trial and error to be best approximated by $D = W \times W$, centered directly under the footing, where W is 40% of the average mean wedge zone depth:

$$W = \frac{0.4}{2}\hat{\mu}_B \tan\left(\frac{\pi}{4} + \frac{\mu_{\phi}}{2}\right), \tag{31}$$

and where μ_{ϕ} is the mean friction angle (in radians) within the zone of influence of the footing, and $\hat{\mu}_B$ is an estimate of the mean footing width obtained by using mean soil properties (μ_c and μ_{ϕ}) in equation (21):

$$\hat{\mu}_B = \frac{I[\alpha_{\mathrm{L}}\hat{L}_{\mathrm{L}} + \alpha_{\mathrm{D}}\hat{L}_{\mathrm{D}}]}{\phi_{\mathrm{g}}\mu_c\mu_{N_c}}. \tag{32}$$

To first order, the mean of N_c is:

$$\mu_{N_c} \simeq \frac{e^{\pi\tan\mu_{\phi}}\tan^2\left(\frac{\pi}{4} + \frac{\mu_{\phi}}{2}\right) - 1}{\tan\mu_{\phi}}. \tag{33}$$

The choice of a square averaging domain is arbitrary. In principle, the domain D should represent the area of soil that directly contributes to the bearing capacity. That is, D would be the area of soil that deforms during failure. Since this area will change, sometimes dramatically, from realization to realization, the above can only be considered a rough empirical approximation. Figure 5 illustrates the location of the averaging domain D relative to the footing centerline.

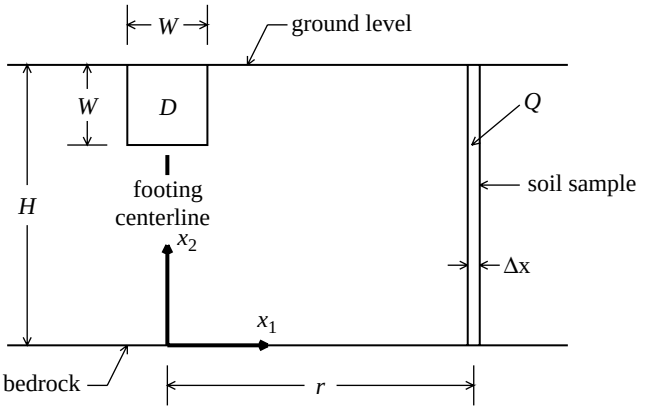

Figure 5. Averaging regions used to predict probability of bearing capacity failure.

Armed with the above information and assumptions, and given the basic statistical parameters of the loads, c, ϕ, the number and locations of the soil samples, and the averaging domain size D, the components of equations (27) and (28) can be computed as follows.

(1) Assuming that the total load L is equal to the sum of the maximum live load, L_{Le}, acting over the lifetime of the structure and the static dead load, L_{D}, i.e. $L = L_{\mathrm{Le}} + L_{\mathrm{D}}$, both of which are random, then

$$\mu_{\ln \mathrm{L}} = \ln(\mu_{\mathrm{L}}) - \frac{1}{2}\ln(1 + V_{\mathrm{L}}^2) \tag{34a}$$

$$\sigma_{\ln \mathrm{L}}^2 = \ln(1 + V_{\mathrm{L}}^2), \tag{34b}$$

where $\mu_{\mathrm{L}} = \mu_{\mathrm{L_e}} + \mu_{\mathrm{D}}$, and V_{L} is the coefficient of variation of the total load defined by

$$V_{\mathrm{L}}^2 = \frac{\sigma_{\mathrm{L_e}}^2 + \sigma_{\mathrm{D}}^2}{(\mu_{\mathrm{L_e}} + \mu_{\mathrm{D}})^2}. \tag{35}$$

(2) With reference to equation (8),

$$\mu_{\ln \hat{c}} = \mathrm{E}\left[\frac{1}{m}\sum_{i=1}^{m}\ln c_i^{\mathrm{o}}\right] = \mu_{\ln c}, \tag{36}$$

$$\sigma_{\ln \hat{c}}^2 \simeq \frac{\sigma_{\ln c}^2}{m^2}\sum_{i=1}^{m}\sum_{j=1}^{m}\rho(\underset{\sim}{x}_i^{\mathrm{o}} - \underset{\sim}{x}_j^{\mathrm{o}}), \tag{37}$$

where $\underset{\sim}{x}_i^{\mathrm{o}}$ is the spatial location of the center of the ith soil sample ($i = 1,2,\ldots, m$) and ρ is the correlation function defined by equation (13). The approximation in the variance arises because correlation coefficients between the local averages associated with observations (in that all tests are performed on samples of some finite volume) are approximated by correlation coefficients between the local average centers. Assuming that $\ln \hat{c}$ actually represents a local average of $\ln c$ over a domain of size $\Delta x \times H$, where Δx

is the horizontal dimension of the soil sample, which, for example, can be thought of as the horizontal zone of influence of a CPT sounding, and H is the depth over which the samples are taken, then $\sigma^2_{\ln\hat{c}}$ is more accurately computed as:

$$\sigma^2_{\ln\hat{c}} = \sigma^2_{\ln c}\gamma(\Delta x, H). \tag{38}$$

See figure 5 for an illustration of the soil sample domain.

(3) With reference to equation (29):

$$\mu_{\ln\bar{c}} = \mathrm{E}\left[\frac{1}{D}\int_{\mathrm{D}} \ln c(\underset{\sim}{x})d\underset{\sim}{x}\right] = \mu_{\ln c}, \tag{39}$$

$$\sigma^2_{\ln\bar{c}} = \sigma^2_{\ln c}\gamma(D), \tag{40}$$

$\gamma(D) = \gamma(W,W)$, as discussed above is defined by equation (14).

(4) Since $\mu_{\hat{\phi}} = \mu_\phi$ (see equation 9), the mean and variance of $\hat{N}_c$ can be obtained using first order approximations to expectations of equation (11) (Fenton and Griffiths 2003) as follows:

$$\mu_{\ln\hat{N}_c} = \mu_{\ln N_c} \simeq \ln\frac{e^{\pi\tan\mu_\phi}\tan^2\left(\frac{\pi}{4}+\frac{\mu_\phi}{2}\right) - 1}{\tan\mu_\phi}, \tag{41}$$

$$\sigma^2_{\ln\hat{N}_c} \simeq \sigma^2_{\hat{\phi}}\left(\frac{d\ln\hat{N}_c}{d\hat{\phi}}|_{\mu\phi}\right)^2 = \sigma^2_{\hat{\phi}}\left[\frac{bd}{bd^2-1}[\pi(1+a)^2d+1+d^2] - \frac{1+a^2}{a}\right]^2, \tag{42}$$

where $a = \tan(\mu_\phi)$, $b = e^{\pi a}$, $d = \tan((\pi/4)+(\mu_\phi/2))$. The variance of $\hat{\phi}$ can be obtained by making use of equation (18):

$$\sigma^2_{\hat{\phi}} \simeq \frac{\sigma^2_\phi}{m^2}\sum_{i=1}^{m}\sum_{j=1}^{m}\rho(\underset{\sim}{x}^0_i - \underset{\sim}{x}^0_j) = \sigma^2_\phi\gamma(\Delta x, H), \tag{43}$$

where $\underset{\sim}{x}^0_i$ is the spatial location of the center of the ith soil observation ($i = 1,2,\ldots,m$). See equation (17) for the definition of σ_ϕ. All angles are measured in radians, including those used in equation (17).

(5) Since $\mu_{\bar{\phi}} = \mu_\phi$ (see equation 30), the mean and variance of $\bar{N}_c$ can be obtained in the same fashion as for $\hat{N}_c$ (in fact, they only differ due to differing local averaging in the variance calculation). With reference to equations 6 and 41:

$$\mu_{\ln\bar{N}_c} = \mu_{\ln\hat{N}_c} = \mu_{\ln N_c}, \tag{44}$$

$$\sigma^2_{\ln\bar{N}_c} \simeq \sigma^2_{\bar{\phi}}\left(\frac{d\ln\bar{N}_c}{d\bar{\phi}}|_{\mu_\phi}\right)^2 = \sigma^2_{\bar{\phi}}\left[\frac{bd}{bd^2-1}[\pi(1+a^2)d+1+d^2] - \frac{1+a^2}{a}\right]^2, \tag{45}$$

$$\sigma^2_{\bar{\phi}} = \sigma^2_\phi\gamma(D) = \sigma^2_\phi\gamma(W,W). \tag{46}$$

See previous item for definitions of a, b, and d. The variance reduction function $\gamma(W,W)$ is defined for two-dimension by equation (14), and equation (17) defines σ_ϕ. All angles are measured in radians.

(6) The covariance between the observed cohesion values and the equivalent cohesion beneath the footing is obtained as follows for $D = W \times W$ and $Q = \Delta x \times H$ (see figure 5):

$$\mathrm{Cov}[\ln\bar{c},\ \ln\hat{c}] \simeq \frac{\sigma^2_{\ln c}}{D^2Q^2}\int_D\int_Q \rho(\underset{\sim}{x}_1 - \underset{\sim}{x}_2)d\underset{\sim}{x}_1 d\underset{\sim}{x}_2 = \sigma^2_{\ln c}\gamma_{DQ}, \tag{47}$$

where γ_{DQ} is the average correlation coefficient between the two areas D and Q. The area D denotes the averaging region below the footing over which equivalent properties are defined, and the area Q denotes the region over which soil samples are gathered. These areas are illustrated in figure 5. In detail, γ_{DQ} is defined by:

$$\gamma_{DQ} = \frac{1}{(W^2\Delta x H)^2} \times\int_{-W/2}^{W/2}\int_{H-W}^{H}\int_{r-\Delta x/2}^{r+\Delta x/2}\int_0^H \rho(\xi_1 - x_1, \xi_2 - x_2)d\xi_2 d\xi_1 dx_2 dx_1, \tag{48}$$

where r is the horizontal distance between the footing centerline and the centerline of the soil sample column. Equation (48) can be evaluated by Gaussian quadrature.

(7) The covariance between $\bar{N}_c$ and $\hat{N}_c$ is similarly approximated by:

$$\mathrm{Cov}\,[\ln\bar{N}_c,\ \ln\hat{N}_c] \simeq \sigma^2_{\ln N_c}\gamma_{DQ}, \tag{49}$$

$$\sigma^2_{\ln N_c} \simeq \sigma^2_\phi\left(\frac{d\ln N_c}{d\phi}|_{\mu\phi}\right)^2 = \sigma^2_\phi\left[\frac{bd}{bd^2-1}[\pi(1+a^2)d+1+d^2] - \frac{1+a^2}{a}\right]^2. \tag{50}$$

Substituting these results into equations (27) and (28) gives:

$$\mu_{\ln Y} = \mu_{\ln L}, \tag{51}$$

$$\sigma^2_{\ln Y} = \sigma^2_{\ln L} + [\sigma^2_{\ln c} + \sigma^2_{\ln N_c}][\gamma(\Delta x, H) + \gamma(W,W) - 2\gamma_{DQ}], \tag{52}$$

which can now be used in equation (25) to produce estimates of p_f. Letting:

$$q = I[\alpha_\mathrm{L}\hat{L}_\mathrm{L} + \alpha_\mathrm{D}\hat{L}_\mathrm{D}], \tag{53}$$

the probability of failure becomes:

$$p_\mathrm{f} = \mathrm{P}[Y > q/\phi_\mathrm{g}] = \mathrm{P}[\ln Y > \ln(q/\phi_\mathrm{g})] = 1 - \Phi\left(\frac{\ln(q/\phi_\mathrm{g}) - \mu_{\ln Y}}{\sigma_{\ln Y}}\right) \tag{54}$$

where Φ is the standard normal cumulative distribution function.

5. Comparison of theory with simulation

To test the proposed theory, a series of $n_{\text{sim}} = 2000$ realizations of a strip footing were simulated (Zhang 2007), for each of a series of soil variability parameters and soil sampling distances, and used to estimate the probability of bearing capacity failure. The simulation-based estimates were then compared to that predicted by the above theory.

In detail, the simulation proceeds as follows.

1. The strength parameters, c and ϕ, of a soil mass are simulated as spatially variable random fields using the local average subdivision (LAS) method (Fenton and Vanmarcke 1990).
2. The simulated soil mass is *virtually* sampled over a column (as in a CPT or SPT sounding) near the footing (see figure 5). Virtual sampling means that the simulated soil values are observed at each of the specified observation points (in this case, over a column of soil 'elements'). No attempt is made here to include the effects of measurement error nor of errors in mapping actual observations, e.g. CPT values, to engineering properties, such as cohesion and friction angle. Thus, the predicted failure probability (either from theory or simulation) will be somewhat unconservative (failure probability increases as measurement error increases). However, both the theory and the simulation treat measurement error in the same way, allowing a consistent comparison between the two.
3. The virtually sampled soil properties are used to estimate the characteristic engineering properties (see equations (8) and (9)).
4. The characteristic soil properties are used to determine $\hat{R}_{\text{u}}$ (see equation (10)) and the design footing width, B, from equation (21).
5. A footing of width B, rounded up to span a whole number of finite elements, is now virtually placed on the simulated soil mass, and a random load having a distribution appropriate to the characteristic loads used in the design is simulated and applied to the

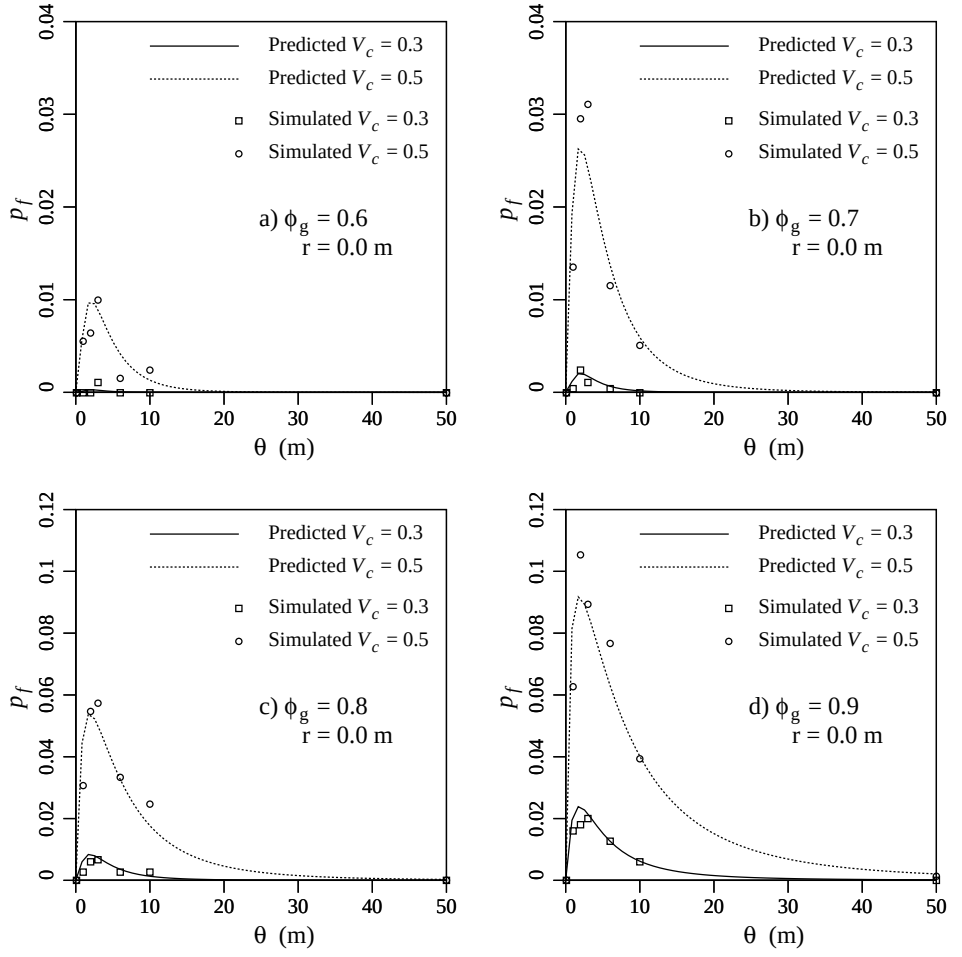

Figure 6. Comparison of theory and simulation-based failure probabilities when sampling directly under the footing ($r = 0$ m) for various resistance factors, ϕ_{g}.

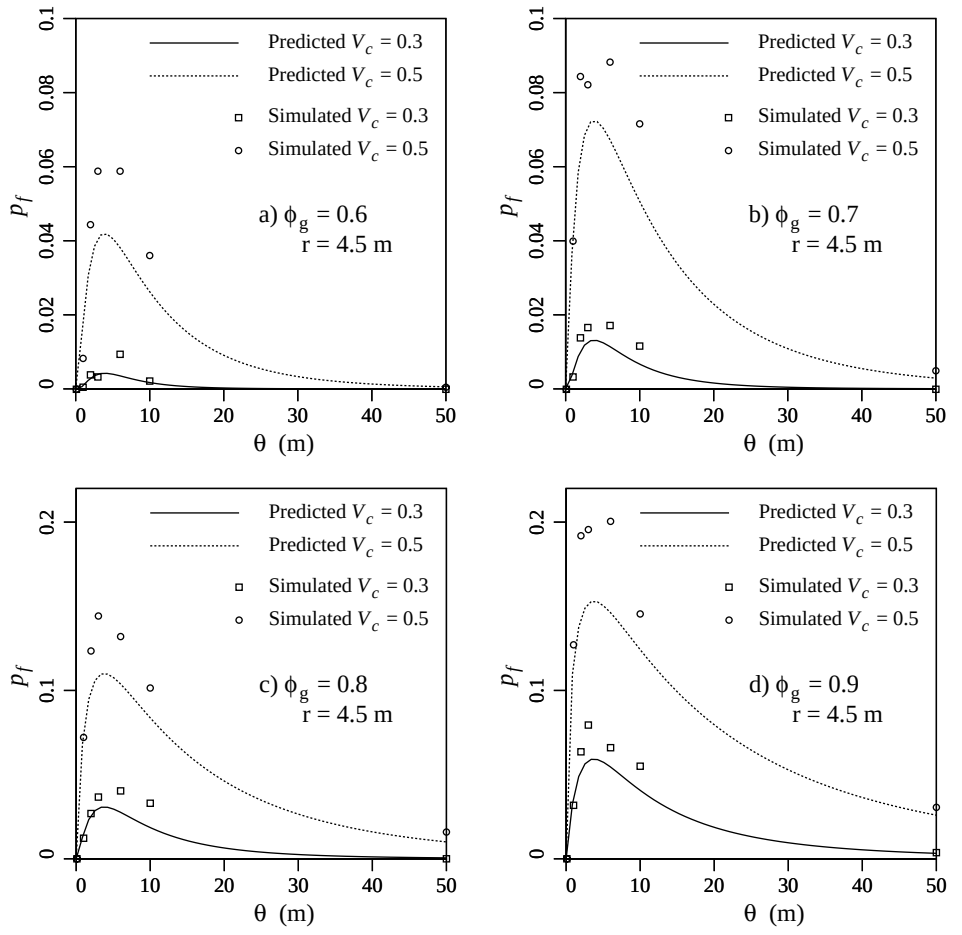

Figure 7. Comparison of theory and simulation-based failure probabilities when sampling near the footing ($r = 4.5$ m) for various resistance factors, ϕ_g.

footing. The response of the soil to the loaded footing is then assessed using the finite element method (Smith and Griffiths 2004) and whether or not the footing experiences a bearing capacity failure is recorded.

6. The entire process from step 1 to step 5 is repeated n_{sim} times. If n_f of these repetitions result in a bearing capacity failure, then the probability of failure, p_f, is estimated as:

$$\hat{p}_f = \frac{n_f}{n_{sim}}. \tag{55}$$

The standard error of the failure probability estimator, $\hat{p}_f$, is $\sigma_{\hat{p}_f} \simeq \sqrt{\hat{p}_f / n_{sim}}$.

The simulated design problem was one of a strip footing supporting loads having means and standard deviations:

$$\mu_{L_e} = 200 \text{ kN/m} \quad \sigma_{L_e} = 60 \text{ kN/m} \tag{56a}$$

$$\mu_D = 600 \text{ kN/m} \quad \sigma_D = 90 \text{ kN/m}. \tag{56b}$$

Assuming bias factors $k_D = 1.18$ (Becker 1996) and $k_{L_e} = 1.41$ (Allen 1975) gives the characteristic loads:

$$\hat{L}_L = 1.41(200) = 282 \text{ kN/m} \tag{57a}$$

$$\hat{L}_D = 1.18(600) = 708 \text{ kN/m}, \tag{57b}$$

and the total factored design load (assuming $I = 1$) is:

$$q = I(\alpha_L \hat{L}_L + \alpha_D \hat{L}_D) = 1.5(282) + 1.25(708) = 1308 \text{ kN/m}. \tag{58}$$

As long as the ratio of dead to live load (assumed to be 3.0 in this study), the coefficients of variation of the load (assumed to be $V_{L_e} = 0.3$ and $V_D = 0.15$), and the characteristic bias factors, k_{L_e} and k_D, are unchanged, the results presented here are independent of the load applied to the strip footing. Minor changes in load ratios, coefficients of variation, and bias factors should not result in significant changes to the probability of bearing failure.

The correlation length, θ, was varied between 0.1 and 50.0 m, and two coefficients of variation of cohesion, V_c, were considered: $V_c = 0.3$ and 0.5. The corresponding coefficients of variation of the friction angle are $V_\phi = 0.20$ ($s = 3$) and $V_\phi = 0.29$ ($s = 5$). The friction angle distribution is assumed to range from $\phi_{min} = 0.1745$ radians (10°) to

$\phi_{max} = 0.5236$ radians (30°). The cohesion was assumed to have constant mean of 100 kPa.

Figures 6–8 illustrate the agreement between theory and simulation for three different sampling locations; $r = 0.0$ m in figure 6, $r = 4.5$ in figure 7, and $r = 9.0$ m in figure 8. As expected, the probability of bearing capacity failure increases as the distance between the footing and the sampling point increases. What this means is that as the understanding of the soil conditions under the footing worsens, the probability of failure increases, all else being held constant.

Figures 6–8 clearly demonstrate the existence of a 'worst case' correlation length, between about 1 and 5 m, where the bearing capacity failure probability reaches a maximum both in the simulations and in the theory. This worst case correlation length is of the same magnitude as the mean footing width ($\hat{\mu}_B = 1.26$ m). The presence of a worst case correlation length can be explained as follows; if the random soil fields are stationary then soil samples yield perfect information, regardless of their location relative to the footing, if the correlation length is either zero or infinity. When the information is perfect, then the probability of a bearing capacity failure goes to zero since the design becomes perfect (assuming that $\phi_g < 1.0$, and that the load bias factors are > 1.0).

When the correlation length is zero, the soil sample will consist of an infinite number of independent 'observations' whose average is equal to the true mean (or true median, if the average is a geometric average). Since the footing also averages the soil properties, the footing 'sees' the same true mean (or true median) value predicted by the soil sample. Thus, the sample information when the correlation length is zero becomes perfect, and so the probability of failure is zero.

At the other end of the scale, when the correlation length goes to infinity, the soil becomes uniform, having the same value everywhere. In this case, any soil sample also perfectly predicts conditions under the footing.

At intermediate correlation lengths, soil samples become imperfect estimators of conditions under the footing, and

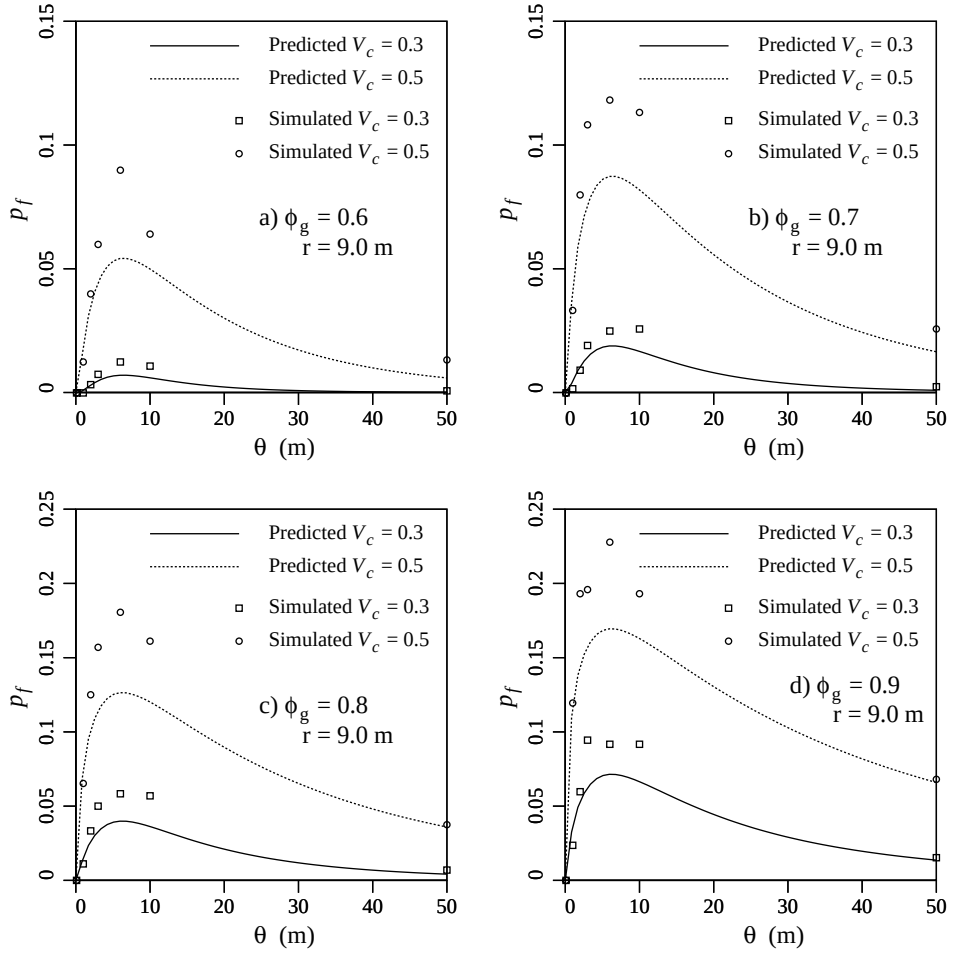

Figure 8. Comparison of theory and simulation-based failure probabilities when sampling at some distance from the footing ($r = 9.0$ m) for various resistance factors, ϕ_g.

so the probability of bearing capacity failure increases. Thus, the maximum failure probability will occur at some correlation length between 0 and infinity. The precise value depends on the geometric characteristics of the problem under consideration, such as the footing width, depth to bedrock, length of soil sample and/or the distance to the sample point. Notice in figures 6–8 that the worst case point does show some increase as the distance to the sample location, r, increases.

The resistance factor, ϕ_g appearing in equation (21), is varied over a range of possible values in figures 6–8. The dependence of the failure probability on the resistance factor suggests that these figures can be used in the reverse direction to determine the resistance factor required to achieve a certain maximum acceptable failure probability. For example, suppose that the maximum acceptable failure probability is 0.01, that $V_c = 0.5$ (and so $V_\phi = 0.29$), and that the worst case correlation length is assumed. In this case, figure 6(a) suggests that $\phi_g = 0.6$ should be used in the LRFD design equation (equation 21). The determination of resistance factors required for various target maximum acceptable failure probabilities, soil variabilities, and site understanding is the topic of a companion paper by Fenton *et al*. (2007).

The failure probabilities are well predicted by the theory when the sampling point is directly below the footing ($r = 0.0$ m). There are some discrepancies for very small probabilities, but this may be largely due to estimator error in the simulations. For example, if $p_f = 0.001$, then the estimator error is $\sigma_{\hat{p}_f} = \sqrt{(0.001)(0.999)2000} = 0.0007$. This means that $\hat{p}_f$ has a coefficient of variation of 70%, which is not very accurate when p_f is as small as 0.001. This means that the simulation cannot be used to validate small probabilities, i.e. probabilities less than about 0.005.

When the sampling location moves away from the footing ($r > 0$), the failure probability becomes somewhat underpredicted at worst case correlation lengths, but still well predicted at small and large scales. This underprediction at intermediate correlation lengths is unconservative, but the theoretical failure probabilities underestimate the simulated probabilities by no less than a factor of about 2/3, which suggests that the theoretical probabilities are in the correct ballpark.

6. Conclusions

This paper presents an analytical technique for estimating the probability of bearing capacity failure of a shallow footing. The theory is compared to simulation and the agreement is very good, especially when the soil is sampled directly under the footing. In other cases, the results are reasonably accurate considering all other sources of uncertainty and typical levels of accuracy in geotechnical calculations.

The theoretical failure probabilities are unconservative in the following ways.

1. Measurement and model errors are not considered in this study. The statistics of measurement errors are very difficult to determine, since the true values need to be known. Similarly, model errors, which relate both the errors associated with translating measured values (e.g. CPT measurements to friction angle values) and the errors associated with predicting bearing capacity by an equation, such as equation (2), to the actual bearing capacity are extremely difficult to measure simply because the true bearing capacity along with the true soil properties are rarely, if ever, known. In the authors' opinion this is the major source of unconservativism in the presented theory. When confidence in the measured soil properties or in the model used is low, the results presented here can still be employed by assuming that the soil samples were taken further away from the footing location than they actually were (e.g. if low-quality soil samples are taken directly under the footing, at $r = 0$, the failure probability corresponding to a larger value of r, say $r = 4.5$ m, should be used).
2. The failure probabilities given by the above theory are underpredicted by a factor of up to about 2/3 when soil samples are taken at some distance from the footing at worst case correlation lengths.

On the other hand, the predicted failure probabilities are conservative in the following ways.

1. c and ϕ are assumed independent, rather than negatively correlated, which leads to a somewhat higher probability of failure and therefore somewhat conservative results. However, the effect of non-zero correlation of c and ϕ was found by Fenton and Griffiths (2003) to be quite minor, so this is not deemed to be a strong conservatism.
2. If the worst case correlation length is assumed due to lack of site specific information, the slight underprediction of the failure probability may actually be more realistic, since it is unlikely that the correlation length of the residual random process at a site (after removal of any mean or mean trend estimated from the site investigation, assuming there is one) will actually equal the 'worst case' correlation length.
3. The soil is assumed weightless in this study. The addition of soil weight, which the authors feel to be generally less spatially variable than soil strength parameters, should reduce the failure probability.
4. More than one CPT, or multiple samples, may be available at the site in the footing region, so that the site understanding may exceed even the $r = 0$ m case

considered here if trends and layering are carefully taken into account.

To some extent the conservative and unconservative factors listed above cancel one another out. In addition, the accuracy of the theory is only as good as the accuracy of the parameters that go into it. For example, the theory depends on knowledge about the mean load, the variance of the soil properties (c and ϕ) and the covariance structure. The worst case correlation length can be used to specify the covariance structure (conservative), but often the variances of the soil properties are only poorly known. In light of this uncertainty, the accuracy of the theoretically predicted failure probability is quite adequate. Thus, the theory can be used to assess the reliability of designs, and more importantly, to aid in the development of reliability-based design codes.

Acknowledgements

The authors would like to thank the National Sciences and Engineering Research Council of Canada, under Discovery Grant OPG0105445, and to the National Science Foundation of the United States of America, under Grant CMS-0408150, for their essential support of this research.

7. Notation

a	$\tan \mu_\phi$
b	$e^{\pi a}$
B	strip footing width
c	cohesion
$\bar{c}$	geometric average of cohesion field over domain D
$\hat{c}$	geometric average of observed (sampled) cohesion values
c_i^o	observed (sampled) cohesion value
d	$\tan\left(\frac{\pi}{4}+\frac{\mu_\phi}{2}\right)$
D	effective soil property averaging domain centered under footing $= W \times W$
D_1	x_1 dimension of the averaging domain D
D_2	x_2 dimension of the averaging domain D
E[·]	expectation operator
$f_L(l)$	probability density function of load
$G_{\ln c}$	standard normal random field (log-cohesion)
G_ϕ	standard normal random field (underlying friction angle)
H	depth to bedrock and depth of assumed soil sample
I	importance factor
k_{Le}	extreme lifetime live load bias factor
k_D	dead load bias factor
L	total true (random) footing load (kN/m)
L_D	true (random) dead load (kN/m)
$\hat{L}_D$	characteristic dead load $= k_D \mu_D$ (kN/m)
L_{L_e}	true (random) maximum live load over design life (kN/m)
$\hat{L}_L$	characteristic live load $= k_{Le}\mu_{Le}$ (kN/m)
m	number of soil observations
n_f	number of failures out of n_{sim} realizations
n_{sim}	number of realizations in a simulation
N_c	N-factor associated with cohesion, which is a function of ϕ
$\bar{N}_c$	effective N-factor associated with cohesion, which is based on an arithmetic average of the friction angle over domain D
$\hat{N}_c$	characteristic N-factor associated with cohesion, which is based on an arithmetic average of the observed friction angles over domain Q (m soil sample observations)
p_f	probability of bearing capacity failure
q_u	ultimate bearing stress
q	factored design load $= I(\alpha_L \hat{L}_L + \alpha_D \hat{L}_D)$
Q	characteristic soil property averaging domain $\Delta x \times H$
r	distance between soil sample and footing center (m)
R_u	ultimate geotechnical resistance (actual, random)
$\hat{R}_u$	ultimate geotechnical resistance based on characteristic soil properties
s	scale factor used in distribution of ϕ
V_c	coefficient of variation of cohesion
V_D	coefficient of variation of dead load
V_L	coefficient of variation of total load
V_{L_e}	coefficient of variation of extreme lifetime load
V_ϕ	coefficient of variation of friction angle
W	side dimension of effective averaging domain D
$\underset{\sim}{x}$	spatial coordinate, (x_1, x_2) in 2-D
$\underset{\sim}{x}_i^0$	spatial coordinate of the center of the ith soil sample
x_i	spatial direction (x_1 or x_2)
Y	true load times ratio of estimated to effective bearing capacity
α_L	live load factor
α_D	dead load factor
Δx	horizontal dimension of soil samples
ϕ	friction angle (radians unless otherwise stated)
ϕ_g	resistance factor
$\bar{\phi}$	arithmetic average of ϕ over domain D
$\hat{\phi}$	arithmetic average of the m observed friction angles
ϕ_{min}	minimum friction angle
ϕ_{max}	maximum friction angle
ϕ_i^0	ith observed friction angle
Φ	standard normal cumulative distribution function
$\gamma(D)$	common variance function giving variance reduction due to averaging over domain D
$\gamma_{\ln c}(D)$	variance function giving variance reduction due to averaging log-cohesion over domain
$\gamma_\phi(D)$	variance function giving variance reduction due to averaging G_ϕ over domain D

γ_{DQ} average correlation coefficient between domains D and Q
μ_c cohesion mean
$\mu_{\ln c}$ log-cohesion mean
$\mu_{\ln \hat{c}}$ mean of the estimate of log-cohesion based on a geometric average of cohesion observations
$\mu_{\ln \bar{c}}$ mean of the effective log-cohesion based on a geometric average of cohesion over domain D
μ_{Nc} mean of N_c
μ_{lnNc} mean of $\ln N_c$
$\mu_{\ln \hat{N}_c}$ mean of $\ln \hat{N}_c$
$\mu_{\ln \bar{N}_c}$ mean of $\ln \bar{N}_c$
μ_{D} mean dead load
μ_{L} mean total load on strip footing (kN/m)
$\mu_{\mathrm{L_e}}$ mean extreme live load over design life
$\mu_{\ln L}$ mean total log-load on strip footing
μ_{ϕ} mean friction angle
$\mu_{\hat{\phi}}$ mean of estimated friction angle
$\mu_{\bar{\phi}}$ mean of effective friction angle in zone of influence under footing
$\mu_{\ln Y}$ mean of $\ln Y$
$\hat{\mu}_B$ estimated mean footing width
θ correlation length of the random fields
$\theta_{\ln c}$ correlation length of the log-cohesion field
θ_{ϕ} correlation length of the G_{ϕ} field
$\rho(\underset{\sim}{\tau})$ common correlation function
$\rho_{\ln c}(\underset{\sim}{\tau})$ correlation function giving correlation between two points in the log-cohesion field
$\rho_{\phi}(\underset{\sim}{\tau})$ correlation function giving correlation between two points in the G_{ϕ} field
σ_c cohesion standard deviation
σ_{D} dead load standard deviation
$\sigma_{\mathrm{L_e}}$ standard deviation of extreme lifetime live load
σ_{L} standard deviation of total load
$\sigma_{\ln L}$ standard deviation of total log-load
$\sigma_{\ln c}$ log-cohesion standard deviation
$\sigma_{\ln \bar{c}}$ standard deviation of $\ln \bar{c}$
$\sigma_{\ln \hat{c}}$ standard deviation of $\ln \hat{c}$
σ_{ϕ} standard deviation of ϕ
$\sigma_{\bar{\phi}}$ standard deviation of $\bar{\phi}$
$\sigma_{\mathrm{lnN_c}}$ standard deviation of $\ln N_c$
$\sigma_{\ln \bar{N}_c}$ standard deviation of $\ln \bar{N}_c$
$\sigma_{\ln \hat{N}_c}$ standard deviation of $\ln \hat{N}_c$
$\sigma_{\ln Y}$ standard deviation of $\ln Y$
$\underset{\sim}{\tau}$ vector between two points in the soil domain
τ_1 horizontal component of the distance between two points in the soil domain
τ_2 vertical component of the distance between two points in the soil domain

References

Allen, D. E., Limit states design – a probabilistic study, *Can. J. Civ. Eng.*, 1975, **36** (2), 36–49.

Becker, D. E., Eighteenth Canadian geotechnical colloquium: Limit states design for foundations. Part II. Development for the National Building Code of Canada, *Can. Geotech. J.*, 1996, **33**, 984–1007.

Cherubini, C., Reliability evaluation of shallow foundation bearing capacity on c', ϕ' soils, *Can. Geotech. J.*, 2000, **37**, 264–269.

Fenton, G. A., Estimation for stochastic soil models, *ASCE J. Geotech. Geoenviron. Eng.*, 1999, **125** (6), 470–485.

Fenton, G. A. and Vanmarcke, E. H., Simulation of random fields via local average subdivision, *ASCE J. Engrg. Mech.*, 1990, **116** (8), 1733–1749.

Fenton, G. A. and Griffiths, D. V., Bearing capacity prediction of spatially random c–ϕ soils, *Can. Geotech. J.*, 2003, **40** (1), 54–65.

Fenton, G. A., Zhang, X. Y. and Griffiths, D. V. (2007). Load and resistance factor design of shallow foundations against bearing failure, *Can. Geotech. J.*, 2007. (submitted)

Griffiths, D. V. and Smith, I. M., *Numerical Methods for Engineers* (2nd edn), 2006 (Chapman & Hall/CRC Press Inc.: Boca Raton, FL).

Meyerhof, G. G., The ultimate bearing capacity of foundations, *Géotechnique*, 1951, **2** (4), 301–332.

Meyerhof, G. G., Some recent research on the bearing capacity of foundations, *Can. Geotech. J.*, 1963, **1** (1), 16–26.

NBCC, *User's Guide – NBC 2005 Structural Commentaries (Part 4 of Division B)* (2nd edn.) 2006 (Ottawa: National Research Council of Canada).

Prandtl, L., Über die Eindringungsfestigkeit (Harte) plastischer Baustoffe und die Festigkeit von Schneiden, *Zeitschr. Angewan. Mathemat. Mech.*, 1921, **1** (1), 15–20.

Smith, I. M. and Griffiths, D. V., *Programming the Finite Element Method* (4th edn), 2004 (John Wiley & Sons: New York).

Sokolovski, V. V., *Statics of Granular Media*, 1965 (Pergamon Press: London, UK).

Terzaghi, K., *Theoretical Soil Mechanics*, 1943 (John Wiley & Sons: New York).

Vanmarcke, E. H., *Random Fields: Analysis and Synthesis*, 1984 (The MIT Press: Cambridge, MA).

Wolff, T. H. Analysis and design of embankment dam slopes: a probabilistic approach, Ph.D. Thesis, 1985 (Lafayette, IN: Purdue University).

Zhang, X. Y. Reliability-based bearing capacity design of shallow foundations, Ph.D. Thesis, 2007 (Halifax, Nova Scotia: Department of Engineering Mathematics and Internetworking, Dalhousie University).